Title: **Partially open crack model for leakage pressure analysis of bolted metal-to-metal flange**

Authors: **M. Beghini, L. Bertini, C. Santus, A. Guglielmo, G. Mariotti**

DOI Link: https://doi.org/10.1016/j.engfracmech.2015.06.005

Partially open crack model for leakage pressure analysis of bolted metal-to-metal flange

M. Beghini[a], L. Bertini[a], C. Santus[a,*], A. Guglielmo[b], G. Mariotti[b]

[a] *University of Pisa. DICI - Department of Civil and Industrial Engineering. Largo L. Lazzarino 2, 56122 Pisa, Italy.*
[b] *General Electric, Oil & Gas. Nuovo Pignone, Via F. Matteucci 2, 50127 Florence, Italy.*

Abstract

Predicting the leakage condition is of primary importance when designing metal-to-metal flanges. The gap between flange surfaces is regarded as a partially open crack with a zero stress intensity factor, then a model based on fracture mechanics is proposed for predicting leakage pressure. An analytical solution was found, with weight function, considering the condition of crack front at the most internal point of the bolt hole. Finite element and experimental tests validated the effectiveness of the model. In addition, the dependencies on the main flange dimensions were investigated and discussed, providing useful guidelines for optimal flange design.

Keywords: Metal-to-metal flange; Leakage pressure; Partially open crack; Weight function.

*Corresponding author: Ciro Santus
Ph. +39 (0)50 2218007, Fax +39 (0)50 2210604.
Email address: ciro.santus@ing.unipi.it (C. Santus)

Nomenclature

LEFM	Linear Elastic Fracture Mechanics.
SIF	Stress Intensity Factor.
WF	Weight Function.
FE	Finite Element method or Finite Element analysis.
K	Mode I SIF.
a	Crack length.
x	Local coordinate.
$h(x,a)$	Weight Function.
a_{o}	Partially open crack length.
$\sigma_{\mathrm{n}}(x)$	Nominal stress distribution.
σ_0, σ_1	Nominal stress parameters.
K_0, K_1	Weight function integrations for uniform and linear nominal stresses.
β_0, β_1	Uniform and linear SIF coefficients.
D_{V}	Vessel diameter.
t_{V}	Vessel wall thickness.
P_{B}	Bolt pitch.
H	Flange half height.
H_{S}	Stud height.
W	Flange width.
Z	Bolt axis position.
d_{H}	Bolt hole diameter.
d_{B}	Bolt stem diameter.
d_{N}	Nut circle diameter.
d_{t}	Stud thread diameter.
d'_{H}	Model equivalent bolt hole diameter.
L	Flange leakage length.
L_{o}	Flange opening length.
σ_{B}	Bolt preload stress.
p	Vessel internal pressure.
F_{B}	Bolt preload force.
F_{p}	Internal pressure opening force.
α	Compressive stress distribution angle across the flange height.
F_1, F_2	Bolt pressure distribution compensation forces.
$\sigma_{\mathrm{n,B}}(x)$	Nominal stress distribution, bolt preload component.
$\sigma_{\mathrm{n,p}}(x)$	Nominal stress distribution, internal pressure component.
$\sigma_{\mathrm{n,B1}}(x)$	Nominal stress distribution with unitary bolt preload stress.
$\sigma_{\mathrm{n,p1}}(x)$	Nominal stress distribution with unitary internal pressure.
$K_{\mathrm{L,B1}}$	SIF with unitary bolt preload stress.
$K_{\mathrm{L,p1}}$	SIF with unitary internal pressure.
C_β	Weight function combination coefficient.
p_{L}	Leakage pressure: the value of the internal pressure that causes leakage.
p'_{L}	Leakage pressure, with no pressure at the partially open flange surfaces.
$p'_{\mathrm{L,max}}$	Maximum leakage pressure, among the investigated vessels.
$p'_{\mathrm{L,FE}}$	Leakage pressure predicted with the FE model.
$\Delta p'$	Relative difference between analytical and FE models.

1. Introduction

Large centrifugal compressor cases are usually manufactured in two halves, connected by a bolted (or studded) flange. Although using a gasket is strictly recommended for pressure vessels [1], this leakage prevention technique cannot be used for the kind of flange investigated here, primarily because the bolted perimeter is open at the two ends in order to allow the shaft to pass through. This flange is usually called *gasketless*, or *metal-to-metal*, and the leakage of the pressurized fluid inside the vessel is prevented by the bolt preload. Bolted flanges have been widely investigated, however most studies are limited to the compact geometry design for connecting pipes [2, 3, 4, 5, 6, 7, 8, 9, 10, 11, 12, 13], while others are dedicated to the deformation behavior of the gasket [14, 15, 16, 17, 18, 19, 20]. Research on flanges is usually focused on the structural stiffness, stress distributions, and the strength optimization of the flange parts, under bolt preload and internal pressure or other external loadings [2, 3, 6, 7, 8, 9, 10, 11, 12, 18, 21, 22, 23, 24, 25, 26, 27, 28, 29]. The main information from the literature, on metal-to-metal flange leakage, regards the following:

1. The leakage rate is notably affected by the flange surface microgeometry [4, 5, 17, 30, 31, 32]:
    - accurate *surface flatness* is required to avoid local contact discontinuity or limitation of the contact pressure;
    - reduced *surface roughness* is recommended in order to prevent micro-leakage;
    - *roughness orientation* not parallel to the main leakage flux direction reduces the leakage rate.
2. The leakage promoted by unavoidable surface unevenness, and/or poor surface roughness, can be reduced by specific sealants (e.g. any silicone based sealant) in order to fill in local irregularities on the surfaces, which would otherwise be difficult to compensate for by metal deformation produced by the bolt tightening [4, 33].
3. The onset of leakage is usually associated with the loss of contact (zero pressure) between the flange mating surfaces [7, 8, 23, 21, 33], or after a critical tensile stress (usually a few MPa) required to break the sealant film [33, 34].
4. Bolt preload scatter, which generates leakage unreliability, is caused by many factors such as uncertainty of the torque wrench relationship to preload force, bolt tightening sequence and subsequent relaxation, and even thermal effects [24, 35, 36, 37, 38].

In conclusion, although the literature is useful in terms of surface preparation, there has been no a physical description of the metal-to-metal flange leakage. We present a model which finds the value of the internal pressure that generates the leakage. This model is based on the equivalence between the flange surfaces and a partially open crack. The flange surfaces are assumed as being plain and initially flat, only deformed by the opening effect of the internal pressure, which is compensated for by tightening the preloaded bolts (or studs). The leakage was modeled as the condition when the opening front reaches the most internal point of the bolt hole, from where the fluid can exit. The use of the weight function technique, after some assumptions on stress distributions, produced a simple and effective analytical model for predicting leakage pressure. The model was successfully verified with finite element simulations on various flange geometries. In addition, from an experimental point of view, preliminarily tests were published on full scale cases [39]. A dedicated scaled mockup was then manufactured and presented in this paper. The results highlight an evident and very accurate validation of the model. Finally, parametric analyses and optimization guidelines are discussed, emphasizing how the proposed model can be an effective engineering tool for metal-to-metal flange design.

2. Analytical model

2.1. LEFM background

The Weight Function (WF) is an analytical technique that can be used within the Linear Elastic Fracture Mechanics (LEFM) theory. The Stress Intensity Factor (SIF) can be efficiently calculated as the integral of the nominal stress times the WF that only depends on geometry. The *nominal* is the stress if the crack itself were

not present, evaluated at the crack surface (or at the crack line for a plane scheme). This integration is numerically very fast or analytical by assuming an approximate WF form which can be integrated. The mode I stress intensity factor K, for an edge crack (plane scheme), can be calculated by the following relationship [40]:

$$K(a) = \int_0^a \sigma_{\mathrm{n}}(x)\, h(x,a)\mathrm{d}x \tag{1}$$

where $h(x,a)$ is the WF for the given crack geometry, x is the local coordinate ranging from zero to the crack size a and $\sigma_{\mathrm{n}}(x)$ is the nominal stress distribution. Equation 1 is valid when the crack is fully open, e.g. if the $\sigma_{\mathrm{n}}(x)$ is entirely tensile from the crack mouth position $x = 0$ to the crack tip position $x = a$. Under a nominal stress distribution with a compressive region the crack can be partially open for a length a_{o} and closed (with crack faces in contact) for the remaining part of its length [41, 42, 43, 44, 45]. An example of this is shown in Fig. 1 where the nominal stress is tensile at the surface, then becomes compressive, and the crack closes before the tip. Without the mode II loading, the stress distribution of the closed part of the crack is equal to that of a continuous (uncracked) body. Therefore, the open crack portion can be regarded as a crack itself with the reduced length a_{o}. The SIF can still be calculated with Eq. 1, for this newly introduced crack, after updating the WF and limiting the domain of integration to a_{o}. A fundamental feature of this study is that the SIF of a partially open crack has to be zero. If the SIF were positive, a tensile (even singular) stress distribution would result at the partially open crack tip, whereas the crack faces are just in contact with each other. A negative SIF is also not possible otherwise the crack faces would be interpenetrating. Accordingly, the WF integral can be set to zero, for the partially open crack length:

$$K(a_{\mathrm{o}}) = \int_0^{a_{\mathrm{o}}} \sigma_{\mathrm{n}}(x)\, h(x,a_{\mathrm{o}})\, \mathrm{d}x = 0 \tag{2}$$

If the nominal stress is imposed, the partially open crack length a_{o} can be regarded as the unknown in Eq. 2. Alternatively, after setting a certain a_{o} length, a component of the nominal stress can be found to solve the equation. This latter approach is implemented in order to find the flange leakage pressure. When the nominal stress distribution $\sigma_{\mathrm{n}}(x)$ is linear, only two integrations are required for the two distributions reported in Fig. 2, which are the uniform and the linearly variable (for example with zero stress at the surface edge) and then the superimposition principle can be applied. The stress distribution self-similitude of both these two load cases leads to a weight function integration expressed as a SIF configuration coefficient times the stress parameter and the $\sqrt{\pi a}$ term, Eq. 3:

$$\begin{aligned} K_0 &= \textstyle\int_0^a \sigma_0\, h(x,a)\mathrm{d}x = \beta_0\, \sigma_0\sqrt{\pi a} \\ K_1 &= \textstyle\int_0^a \sigma_1\, x/a\, h(x,a)\mathrm{d}x = \beta_1\, \sigma_1\sqrt{\pi a} \end{aligned} \tag{3}$$

The coefficients for the two configurations reported in Fig. 2 are:

$$\begin{aligned} \beta_0 &= 1.1215 \\ \beta_1 &= 0.6820 \end{aligned} \tag{4}$$

The reported coefficients can be deduced as a special case of the WF proposed in [40] and also in [46, 47] which are valid after assuming boundary and loads as remote, i.e. an edge crack in a half-plane. Equations 3, 4 can be equally used even for a partially open crack just by replacing a with a_{o} and with σ_1 being the nominal stress at $x = a_{\mathrm{o}}$. Since only linear stress distributions were assumed, these two WF integrations suffice for the purpose of our model. More specific weight function forms could be provided for future analyses. However, very accurate results were already obtained, as confirmed by the finite element comparison and the experimental validation reported below.

2.2. Bolted metal-to-metal flange leakage model

The flange investigated has bolts distributed along a straight line profile, Fig. 3 (a). This flange can be either with bolts or with studs, Figs. 3 (b) and (c). The geometry parameters are: D_V vessel diameter, t_V vessel wall thickness, P_B bolt pitch, H flange half height, H_S stud height (only for stud geometry), W flange width, Z bolt axis position, d_H bolt (or stud) hole diameter, d_B bolt (or stud) stem diameter, and d_N nut circle diameter. This flange geometry is different from the usual compact flange for pipes, where the profile curvature radius is quite small compared to the flange width and height. Our model can also be developed for small flanges, however, the present paper results are limited to the half-plane crack solution which is consistent with the bolt straight line profile. This study is based on the similitude between the flange contact interface and an edge partially open crack. The leakage condition is when the partially open length L_o equals the flange length L, hereafter referred to as the leakage length, Fig. 4. After reaching this situation the pressurized fluid can exit the vessel through the bolt hole and eventually through the bolt thread. This leakage assumption follows Galai and Bouzid [13], who investigated the flange surface separation specifically at the bolt circle. In accordance with the WF approach, the leakage onset can be stated as zero SIF of a length L partially open crack, Eq. 5:

$$K(L) = \int_0^L \sigma_n(x)\, h(x,L)\mathrm{d}x = 0 \tag{5}$$

The flange interface nominal stress $\sigma_n(x)$ has two components: the stress distribution generated by the bolt preload $\sigma_{n,B}(x)$ and the stress generated by the internal pressure $\sigma_{n,p}(x)$. Since $\sigma_{n,B}(x)$ is proportional to the bolt preload F_B and $\sigma_{n,p}(x)$ is proportional to the internal pressure p, the flange nominal stress can be written as:

$$\sigma_n(x) = \sigma_B\ \sigma_{n,B1}(x) + p\ \sigma_{n,p1}(x) \tag{6}$$

where the bolt preload stress is defined as: $\sigma_B = F_B/(\frac{\pi}{4} d_B^2)$, and $\sigma_{n,B1}$ is the flange stress distribution generated by the unitary bolt preload stress σ_B (without internal pressure) and $\sigma_{n,p1}$ is the unitary internal pressure flange stress distribution, without bolt preload, and assuming bonded flange surfaces to allow tensile stress. The nominal unitary stress distributions $\sigma_{n,B1}(x), \sigma_{n,p1}(x)$ are dimensionless, while σ_B and p have a stress unit (e.g. MPa or ksi). The leakage condition Eq. 5 can be rewritten as:

$$\sigma_B K_{L,B1} + p_L K_{L,p1} = 0 \tag{7}$$

where p_L is the leakage pressure and $K_{L,B1}$ and $K_{L,p1}$ are unitary SIFs obtained as the integrations of the bolt preload and pressure unitary nominal stress distributions, respectively, Eq. 8:

$$\begin{aligned} K_{L,B1} &= \textstyle\int_0^L \sigma_{n,B1}(x)\, h(x,L)\mathrm{d}x \\ K_{L,p1} &= \textstyle\int_0^L [\sigma_{n,p1}(x) + 1]\, h(x,L)\mathrm{d}x \end{aligned} \tag{8}$$

The unit of $K_{L,B1}$ and $K_{L,p1}$ is the square root of a length (e.g. $\sqrt{\mathrm{m}}$), the same unit as the WF. The second of Eq. 8 also takes into account the effect of the pressurized fluid inside the partially open flange, as the fluid immediately fills the open gap between the deformed flange surfaces, Fig. 4. This pressurization introduces a further term that can be easily included in the WF calculation by integrating the fluid pressure times the WF kernel [48]. A unit term is therefore added to $\sigma_{n,p1}(x)$ being $K_{L,p1}$ calculated with the unitary internal pressure.

In order to reduce the entire problem to a bi-dimensional scheme, the flange geometry was approximated to a plane configuration reproducing the bolt hole sequence as a continuous slot, Fig. 5. The dimension d'_H was introduced and calculated by imposing the equivalent area of the slot, Eq. 9:

$$d'_H = \frac{\pi\, d_H^2}{4\, P_B} \tag{9}$$

By following the approach reported in many machine design textbooks (e.g. Shigley [49]) the flange contact pressure, generated by the bolt preload, was assumed to be distributed over a double conical volume extending from the nut base. We approximated the bolt array to a plane scheme and then the bolt preload conical pressure

was reduced to a trapezoidal distribution, in line with this plane geometry assumption. The bolt compressive region is usually larger than the flange surface width W and the axis position of the bolt is typically very close to the inner side of the vessel. The pressure distribution outside the contact (equivalent to the forces F_1, F_2) is redistributed over the flange surface width, and then superimposed on the trapezoidal distribution, thus obtaining the contact pressure $\sigma_{\mathrm{n,B}}(x)$, reported in Fig. 6 (a). The nominal stress distribution at the flange interface, generated by the internal pressure, was evaluated by considering normal stress and bending (linear stress distribution) and again imposing the load equivalence. Figure 6 (b) shows the stress distribution obtained from the internal pressure opening force: $F_{\mathrm{p}} = p\ P_{\mathrm{B}} D_{\mathrm{V}}/2$ by assuming its axis aligned with the mid plane of the vessel wall thickness. Figure 6 shows the stresses at the internal diameter position and at the leakage length, generated by the bolt preload and the internal pressure: $\sigma_{\mathrm{n,B}}(0), \sigma_{\mathrm{n,B}}(L), \sigma_{\mathrm{n,p}}(0), \sigma_{\mathrm{n,p}}(L)$. The unitary stresses can be easily obtained as:

$$\begin{aligned} \sigma_{\mathrm{n,B1}}(0) &= \frac{\sigma_{\mathrm{n,B}}(0)}{\sigma_{\mathrm{B}}}, \quad \sigma_{\mathrm{n,B1}}(L) = \frac{\sigma_{\mathrm{n,B}}(L)}{\sigma_{\mathrm{B}}} \\ \sigma_{\mathrm{n,p1}}(0) &= \frac{\sigma_{\mathrm{n,p}}(0)}{p}, \quad \sigma_{\mathrm{n,p1}}(L) = \frac{\sigma_{\mathrm{n,p}}(L)}{p} \end{aligned} \tag{10}$$

These unitary stresses $\sigma_{\mathrm{n,B1}}(0), \sigma_{\mathrm{n,B1}}(L)$ and $\sigma_{\mathrm{n,p1}}(0), \sigma_{\mathrm{n,p1}}(L)$ can be calculated by the procedure reported in the appendix, which implements the stress distribution assumptions introduced above. Since both stress distributions are assumed as linear across the leakage length L, the WF integrations in Eq. 8 can be solved with the unitary stresses according to the results reported in Eq. 3. Unitary bolt preload and pressure SIFs are calculated as the sum of two terms, uniform and linear:

$$\begin{aligned} K_{\mathrm{L,B1}} &= \beta_0\ \sigma_{\mathrm{n,B1}}(0)\sqrt{\pi L}\ + \beta_1\ [\sigma_{\mathrm{n,B1}}(L) - \sigma_{\mathrm{n,B1}}(0)]\sqrt{\pi L} \\ K_{\mathrm{L,p1}} &= \beta_0\ [\sigma_{\mathrm{n,p1}}(0) + 1]\sqrt{\pi L} + \beta_1\ [\sigma_{\mathrm{n,p1}}(L) - \sigma_{\mathrm{n,p1}}(0)]\sqrt{\pi L} \end{aligned} \tag{11}$$

The leakage pressure can be obtained by solving Eq. 7 after introducing Eq. 11 unitary SIFs:

$$p_{\mathrm{L}} = \sigma_{\mathrm{B}} \frac{|\sigma_{\mathrm{n,B1}}(0)| + C_\beta\ |\sigma_{\mathrm{n,B1}}(L)|}{\sigma_{\mathrm{n,p1}}(0) + C_\beta\ \sigma_{\mathrm{n,p1}}(L) + C_\beta + 1} \tag{12}$$

It is worth noting that $\sigma_{\mathrm{n,B}}$ stresses (as well as $\sigma_{\mathrm{n,B1}}$) are negative, thus the absolute values are required here. Alternatively, they could be introduced with a positive sign regarding them as pressures. The coefficient C_β is a combination of the SIF factors β_0, β_1:

$$C_\beta = \frac{\beta_1}{\beta_0 - \beta_1} = 1.552 \tag{13}$$

A different leakage pressure prediction result is obtained if the fluid pressure penetration is not taken into account, by removing the unit term in the second of Eq. 11:

$$p'_{\mathrm{L}} = \sigma_{\mathrm{B}} \frac{|\sigma_{\mathrm{n,B1}}(0)| + C_\beta\ |\sigma_{\mathrm{n,B1}}(L)|}{\sigma_{\mathrm{n,p1}}(0) + C_\beta\ \sigma_{\mathrm{n,p1}}(L)} \tag{14}$$

The former result p_{L} is the actual leakage pressure, since fluid penetration in the flange gap is unavoidable. The latter result p'_{L} is still useful e.g. for comparisons with finite element simulations (as reported in the next section) where the gap pressurization is not modeled. Obviously, p'_{L} is higher than p_{L} since the penetrated fluid has a further detrimental effect of tearing apart the flange surfaces.

More complex nominal stress distributions rather than just linear could also be considered. A numerical integration with a generic weight function (e.g. Beghini et al. [40]) would give the unitary bolt preload and pressure SIFs: $K_{\mathrm{L,B1}}, K_{\mathrm{L,p1}}$ and the leakage pressure p_{L} could be solved from Eq. 7, however not resulting an explicit form as Eq. 12.

3. Finite element model validation

The Finite Element (FE) modeling of threaded connections and bolted flanges has been widely investigated, as summarized in Mackerle's reviews [50, 51, 52]. Some of these studies have focused on the tightening process [36] and the bolt-up sequence of a flanged connection [37, 53]. The stiffness of bolted joints was investigated in [54, 55, 56, 57, 58] and the bolt self-loosening was examined in [59, 60, 61]. Recent analyses of flanged joints have proposed FE simulations to investigate the contact pressure distributions between the two flange mating surfaces [2, 10, 62]. By following the guidelines derived from the literature, a parametric FE model was implemented. ANSYS software was used with solid three-dimensional 8-node elements with surface-to-surface Contact & Target placed at the flange interface. The total number of elements was approximately 160000. Although the flange material was modeled as linear elastic structural steel (Young's modulus 205 GPa and Poisson's ratio 0.3), the analysis was nonlinear because of the unilateral contact of the flange. As shown in Fig. 7 (a), the modeled portion was limited to half of the bolt pitch having the flange cyclic symmetry. The constraints and loads applied to the model are:

- Symmetry at the axial mid plane in order to model just one flange side.
- Further symmetry with respect to a plane perpendicular to the case axis at the position of the bolt or the stud.
- Zero relative longitudinal displacement on the other side of the FE model.
- Bolt (or stud) preload obtained by imposing a separation between the lower surface of the nut and the upper surface of the flange.
- Internal pressure applied to the inner vessel surfaces.
- Axial load, caused by the internal pressure acting on the lateral surfaces of the vessel, uniformly distributed on the non-fixed section plane.

The bolt separation displacement to induce preload was preliminarily calculated by a linear analysis to find the overall stiffness of the flange. An arbitrary interference value was inputted, the bolt force obtained as output, and their ratio calculated. The specific separation value was given as the ratio between the bolt preload to be imposed and the flange stiffness. The compressive zone induced by bolt preload widens from the nut (or the bolt head) across the flange height by an angle α. According to the literature, α ranges from 30° to 45° both for bolts and studs [49, 63, 64]. This angle is also a parameter of the analytical model, as reported in the appendix. An intermediate value $\alpha = 35°$ was verified to show the best accurate comparative results between the analytical and the FE models, and is in line with the simulated compressive stress distribution, Fig. 7 (b). The FE contact pressure at the flange interface and the comparison with the model is reported in Fig. 8 (a). FE analysis overcomes any stress distribution assumption while the model is limited to a linear spline. However, the overall trend of the contact pressure is well reproduced and the trapezoidal distribution, and also the asymmetry due to the limited flange width, are evident. The internal edge of the flange is merely a sharp notch of a solid structure, thus a singular stress distribution appears. This singularity vanishes if tangent contours are introduced in order to replace the sharp notch with a rounded profile. Accurate prediction and the sharp notch singularity issue are also evident in terms of the stresses induced by the internal pressure, Fig. 8 (b). Being this flange stress component tensile, the latter validation was obtained with bonded contact FE model. The sharp notch stress concentration had a limited consequence on the predicted leakage pressure, mainly because it acts similarly on both bolt preload and internal pressure stress components.
The FE model leakage prediction was found by increasing the internal pressure, with a significant number of small steps, and monitoring the contact elements with imposed unilateral behaviour. Consistently to the analytical model, the leakage condition was assumed when the opening front reached the inner point of the bolt hole circle. Figure 9 shows the flange contact and its opening at different internal pressure increments. A rapid shift of the front was observed after reaching a threshold pressure, thus the uncertainty associated with the FE

model result was quite small. Several vessel geometries were investigated, with different sizes and dimensional ratios, reproducing actual centrifugal compressor cases. The FE model leakage pressure $p'_{L,FE}$ and the analytical model p'_L are reported as normalized values in Table 1. The leakage pressure p'_L, without the effect of the fluid inside the flange gap, can be compared to the FE model results where the flange surfaces were not loaded by the pressure. The relative difference $\Delta p'$ was never larger than a few percentage points and the correlation coefficient between the two models was $R^2 = 0.996$, hence the approximations introduced in the model were acceptable in terms of result accuracy, at least in the considered range of geometry parameters that are typical of actual vessel flanges. The ratio between leakage pressures p_L and p'_L was also calculated and reported for each vessel in Table 1. This ratio was shown to weakly depend on the geometry and its value is approximately 0.9. A wide range of leakage pressure was found, as reported in the table. One of the main influencing parameters was the vessel diameter D_V. A large diameter generated high opening force F_p, hence the leakage pressure was low, whereas higher p'_L, p_L were obtained with smaller vessel diameters.

4. Experimental validation

The successful validation with FE analyses confirmed the ability of our model to predict the internal pressure that drives the open front up to the bolt hole circle. However, the effect of the unevenness of the flange surfaces (not perfect flatness and surface roughness) is obviously not considered in the simulations. We designed an experimental setup specifically to reproduce a small scale flanged vessel with bolts. The size of the vessel was approximately 300 mm and the tests were performed in a laboratory environment, Fig. 10 (a). In order to efficiently detect the leakage, colored water was used as an internal fluid, instead of a gas. Measuring the bolt (or stud) preload is critical. The use of strain gauges attached to the bolt stem is the most accurate and reliable solution for bolt preload monitoring [7, 11, 12, 15]. Two couples of strain gauges (grids at $0° - 90°$) were attached to each bolt in accordance with the full-bridge configuration, Fig. 10 (b), to neutralize any bending and only measure the axial tensile load with an amplification coefficient: $2(1+\nu) = 2.6$, where $\nu = 0.3$ is the bolt steel Poisson's ratio. The load measurement of each bolt with strain gauges was preliminarily calibrated with a tensile testing machine. Several loads were applied to all the instrumented bolts and the corresponding strain gauge readings saved. Before the pressurization tests, these values were replicated in order to be able to set accurate preloads. After wrenching the bolt preload tended to slightly decrease within a few percentage points, as is usual for bolted connections. The bolts were retightened until stable strain gauge measures were obtained, as close as possible to the values recorded during the tensile test calibration. This relaxation correction procedure lasted a few minutes and the resulting strain gauge discrepancy, with respect to the reference, was within a range of $\pm 2\%$. The testing region was limited to a small portion of the flange perimeter. The strain gauges were applied only to four bolts in the middle of one longer side, Fig. 10 (a). The preload applied to the other bolts, controlled with a torque wrench, was substantially larger to avoid leakage in a region with preloads not accurately known, and the transition from the central leakage bolts was gradual.

After setting the bolt preloads, the colored water was introduced inside the vessel and pressurized with a hand pump. The liquid pressure was measured with an analog pressure sensor and an ordinary manometer was also used to double-check the measurement. The vessel was slowly pressurized until the first leakage drop was detected. First the mass of a single water drop was measured, then the leakage flow rate was valued by measuring the number of drops within 10 minutes. During the leakage, the internal pressure decreased and consequently the leakage rate also reduced. The test was continued until zero leakage and a stable internal pressure condition was found. Although the measurement of the flow rate may not be very accurate, the aim of the experiment was simply to detect a vanishingly small leakage rate. The corresponding internal pressure was assumed as the experimental result, which was then compared to the analytical model p_L. Leakage tests were carried out for bolt preloads: $10, 20, 30, 40$ kN and for each preload, two tests were performed. The measured leakage rates and the detection of the leakage pressures are reported in Fig. 11. Figure 12 shows the comparison between the experimental tests and the model. It is evident how the experimental data were very close to the prediction and that the difference between p_L and p'_L was noticeably larger than the discrepancy of the experimental tests, confirming the postulated mechanism of fluid penetration inside the flange gap.

The flatness of the flange surfaces was detected, before the tests, with a digital altimeter Mauser Capax 2000. At the bolt holes of the leakage zone the flatness error was approximately $2-3$ μm considering the contributions of both surfaces. Preliminarily tests with a flatness error up to 25 μm produced notably lower leakage pressures, approximately half the values obtained with ground surface finishing as shown here. This initial experiment clearly showed how essential the flatness of the flange surfaces is.
The tests shown in Fig. 12 were performed without any sealing, but a silicone based sealant is recommended at the flange interface. A final test was also performed after the sealant had been applied and leakage pressure increased considerably. The highly deformable sealing film compensates for the micrometric deformation due to the pressurization. We hypothesize that the effect of the sealing is more pronounced under small scale testing. Full scale testing with sealing were previously performed in industry and a reasonable agreement was found with the model prediction [39]. Large scale flange surface displacements are much higher than that the mockup shown here, hence not easily compensated for by a thin sealing layer.

5. Parametric analysis

The effect of geometry parameters on the leakage pressure can be easily investigated, with the proposed analytical model, by using an electronic worksheet or implementing a short script in any programming language. In contrast, FE analyses would require cumbersome mesh rebuilding and a nonlinear solution for any parametric iteration. This section reports a sensitivity analysis of the main parameters. According to Eq. 12, the leakage pressure and the bolt preload are linearly related. This linear dependency was less evident from the FE point of view. The nonlinearity due to the contact actually has no effect on the relation between bolt preload and leakage pressure, since the contact region is fixed by assuming the open front at the bolt hole circle. Obviously, a few percentage points preload drop implies a similar effect on the leakage pressure. In addition, an increase in σ_{B}, e.g. with a higher strength steel bolt, proportionally improves the leakage pressure of the flange. Using the bolt preload force, rather than the bolt preload stress, can be misleading. In order to exploit the linearity between preload and leakage pressure, a larger bolt size appears deceptively useful to increase the preload force. In fact, a larger bolt diameter results in a higher axis position and higher bolt pitch, which are both detrimental for the leakage pressure, as shown below.
Geometry parametric analyses are reported in Fig. 13 regarding the vessels 3, 6, 8 in Tab. 1. Bolt axis position Z, bolt pitch P_{B}, flange width W and flange height H were investigated. These parameters were reported as dimensionless after dividing by their default values for each the three vessels. The bolt axis position Z has a significant effect on the leakage performance. If the bolt axis is distant from the vessel inner surface (large value of Z), the absolute value of term $\sigma_{\mathrm{n,B}}(0)$ is low because the bolt pressure distribution on the flange interface decreases away from the bolt axis. As a consequence, the higher the Z distance, the lower the leakage pressure p_{L}. This trend can be quantitatively assessed using the proposed model. Results for the three vessels investigated are reported in Fig. 13 (a) where Z larger than the design values are reported. Clearly, the best configuration is obtained with the smallest possible Z. The leakage pressure is also quite sensitive to bolt pitch. A larger bolt pitch produces a lower leakage pressure because the total bolt closure force is distributed on a larger surface and thus the terms $\sigma_{\mathrm{n,B}}(0), \sigma_{\mathrm{n,B}}(L)$ decrease. Figure 13 (b) shows the leakage pressure sensitivity to the bolt pitch, for the same three vessels, by taking into account lower and higher values with respect to the design bolt pitch of each vessel. The bolt pitch should also be reduced as much as possible, the minimum bolt pitch is related to the nut diameter and the space required for a tool. The leakage pressure initially increases with the flange width, but it is almost insensitive after a certain size of W, Fig. 13 (c). If the flange width is small, similar portions of bolt compression load F_1, F_2 fall outside the flange width. If the flange width is large the load portion opposite the internal side (F_2) vanishes, thus a more asymmetric pressure redistribution results and the terms $\sigma_{\mathrm{n,B}}(0), \sigma_{\mathrm{n,B}}(L)$ increase. After the minimum size for which $F_2 = 0$, a further increase in the flange width does not produce any significant effect. Finally, the sensitivity of the leakage pressure on the (half) flange thickness H is quite limited, Fig. 13 (d). The nominal stress distribution produced by the internal pressure is not affected by the flange height, and the redistribution (F_1, F_2) mitigates the flange height effect also about the bolt preload. The flange thickness can thus be considered a secondary variable in terms of the pressure leakage design. Nevertheless, very small

flange thickness would produce flexible plates, affecting the leakage pressure, whereas this is not considered in the model given that the flange section is assumed as a half-plane.

6. Conclusions

The proposed analytical model for predicting flange leakage pressure is based on the similitude between the flange interface and a plane edge partially open crack. The zero mode I stress intensity factor condition was imposed by means of the weight function technique, and an analytical model was derived. The main findings of this study are:

- One of the main advantages of this fracture mechanics similitude is that it is based on the knowledge of nominal stresses alone, thereby avoiding finite element nonlinear calculations.
- A finite element three-dimensional nonlinear model was implemented to validate the prediction of the leakage pressure. The analytical and the validating finite element models were compared on several vessel geometries and the results were very similar with the maximum relative difference limited to a few percentage points.
- Small scale experimental tests confirmed that the model predicts leakage pressure very accurately. The flange surfaces were ground finished before the tests to reduce the flatness error up to a few microns in the bolt region. The surface roughness and flatness can have a significant role on the leakage performance of the metal-to-metal flange. However, these effects cannot be explained with our model, which assumes that surfaces are perfectly flat.
- The analytical model can be quickly and efficiently used for geometry sensitivity analysis. A parametric study was performed for different sized vessels by varying a few important geometry dimensions, and analyzing their influence on the predicted leakage pressure. This analysis showed that the leakage pressure:
  - obviously is proportional to the preload stress, thus bolt preload uncertainty directly affects the vessel leakage performance;
  - decreases by increasing the bolt axis distance and also by increasing the bolt pitch, and these results highlight that these two distances should be kept as low as possible;
  - is only marginally affected by the flange height and width after certain sizes.

This fracture mechanics approach is limited here to a linear bolt pattern. However, dedicated weight function solutions could be proposed and the approach extended to any other bolt profile, for example with a high curvature as circular compact flanges or flange corners.

References

[1] EN 13445-3. Unfired pressure vessels, Part 3: Design (2012).

[2] D. Nash, J. Spence, A. Tooth, M. Abid, D. Power, A parametric study of metal-to-metal full face taper-hub flanges, International Journal of Pressure Vessels and Piping 77 (13) (2000) 791–797, DOI: 10.1016/S0308-0161(00)00071-5.

[3] D. Nash, M. Abid, Combined external load tests for standard and compact flanges, International Journal of Pressure Vessels and Piping 77 (13) (2000) 799–806, DOI: 10.1016/S0308-0161(00)00072-7.

[4] F. Kirkemo, Design of compact flange joints, in: American Society of Mechanical Engineers, Pressure Vessels and Piping Division (Publication) PVP, Vol. 433, 2002, pp. 91–104, vancouver BC, Canada, Paper 1087.

[5] D. Nash, M. Abid, Surface sensitivity study of non-gasketed flange joint, Proceedings of the Institution of Mechanical Engineers, Part E: Journal of Process Mechanical Engineering 218 (4) (2004) 205–212, DOI: 10.1243/0954408042467007.

[6] M. Abid, D. Nash, A parametric study of metal-to-metal contact flanges with optimised geometry for safe stress and no-leak conditions, International Journal of Pressure Vessels and Piping 81 (1) (2004) 67–74, DOI:10.1016/j.ijpvp.2003.11.012.

[7] M. Abid, Determination of gasketed and non-gasketed flanged pipe joint's capacity subjected to combined loading: an experimental approach, International Journal of Mechanics and Materials in Design 2 (1–2) (2005) 35–47, DOI: 10.1007/s10999-005-0519-6.

[8] M. Abid, Determination of safe operating conditions for non-gasketed flange joint under combined internal pressure and temperature, International Journal of Mechanics and Materials in Design 2 (1–2) (2005) 129–140, DOI: 10.1007/s10999-005-4447-2.

[9] M. Abid, S. Iqbal, S. Khushnood, Nonlinear Finite Element Analysis of Gasketed Flange Joints under Combined Internal Pressure and Different Thermal Loading Conditions, Failure of Engineering Materials & StructuresCode Code 50 (2007) 217–228.
[10] D. Joshi, P. Mahadevan, A. Marathe, A. Chatterjee, Unimportance of geometric nonlinearity in analysis of flanged joints with metal-to-metal contact, International Journal of Pressure Vessels and Piping 84 (7) (2007) 405–411, DOI: 10.1016/j.ijpvp.2007.03.004.
[11] M. Abid, A. Awan, D. Nash, Stamina of a non-gasketed flange joint under combined internal pressure and axial loading, Proceedings of the Institution of Mechanical Engineers, Part E: Journal of Process Mechanical Engineering 222 (3) (2008) 143–155, DOI: 10.1243/09544089JPME212.
[12] M. Abid, A. Awan, D. Nash, Performance of a Nongasketed Flange Joint under Combined Internal Pressure and Bending Loading, Journal of Engineering Mechanics 136 (12) (2010) 1519–1527, DOI: 10.1061/(ASCE)EM.1943-7889.0000191.
[13] H. Galai, A.-H. Bouzid, Analytical Modeling of Flat Face Flanges With Metal-to-Metal Contact Beyond the Bolt Circle, Journal of Pressure Vessel Technology, Transactions of the ASME 132 (6) (2010) 0612071–0612078, DOI: 10.1115/1.4001655.
[14] E. Roos, H. Kockelmann, R. Hahn, Gasket characteristics for the design of bolted flange connections of metal-to-metal contact type, International Journal of Pressure Vessels and Piping 79 (1) (2002) 45–52, DOI: 10.1016/S0308-0161(01)00127-2.
[15] T. Sawa, N. Ogata, T. Nishida, Stress Analysis and Determination of Bolt Preload in Pipe Flange Connections With Gaskets Under Internal Pressure, Journal of Pressure Vessel Technology, Transactions of the ASME 124 (4) (2002) 385–396, DOI: 10.1115/1.1511736.
[16] A.-H. Bouzid, M. Derenne, Analytical Modeling of the Contact Stress With Nonlinear Gaskets, Journal of Pressure Vessel Technology, Transactions of the ASME 124 (1) (2002) 47–53, DOI: 10.1115/1.1426084.
[17] J. Arghavani, M. Derenne, L. Marchand, Effect of Surface Characteristics on Compressive Stress and Leakage Rate in Gasketed Flanged Joints, The International Journal of Advanced Manufacturing Technology 21 (10–11) (2003) 713–732, DOI: 10.1007/s00170-001-1120-2.
[18] M. Abid, B. Ullah, Three-dimensional nonlinear finite-element analysis of gasketed flange joint under combined internal pressure and variable temperatures, Journal of Engineering Mechanics 133 (2) (2007) 222–229, DOIi: 10.1061/(ASCE)0733-9399(2007)133:2(222).
[19] M. M. Krishna, M. Shunmugam, N. S. Prasad, A study on the sealing performance of bolted flange joints with gaskets using finite element analysis, International Journal of Pressure Vessels and Piping 84 (6) (2007) 349–357, DOI: 10.1016/j.ijpvp.2007.02.001.
[20] A.-H. Bouzid, H. Galai, A New Approach to Model Bolted Flange Joints With Full Face Gaskets, Journal of Pressure Vessel Technology, Transactions of the ASME 133 (2) (2011) art. no. 021203, DOI: 10.1115/1.4001920.
[21] M. Abid, D. Nash, Comparative study of the behaviour of conventional gasketed and compact non-gasketed flanged pipe joints under bolt up and operating conditions, International Journal of Pressure Vessels and Piping 80 (12) (2003) 831–841, DOI: 10.1016/j.ijpvp.2003.11.013.
[22] A. Shah, I. Korovaichuk, T. Kovacevich, J. Schreiber, Stirling convertor fasteners reliability quantification, in: Collection of Technical Papers - 3rd International Energy Conversion Engineering Conference, 1, 2005, pp. 53–60.
[23] M. Abid, Determination of safe operating conditions for gasketed flange joint under combined internal pressure and temperature: A finite element approach, International Journal of Pressure Vessels and Piping 83 (6) (2006) 433–441, DOI: 10.1016/j.ijpvp.2006.02.029.
[24] M. Abid, D. Nash, Structural strength: Gasketed vs non-gasketed flange joint under bolt up and operating condition, International Journal of Solids and Structures 43 (14–15) (2006) 4616–4629, DOI:10.1016/j.ijsolstr.2005.06.078.
[25] P. Jolly, L. Marchand, A 3D regression surface for the room temperature tightness gasket data reduction and bolt load design, International Journal of Pressure Vessels and Piping 85 (7) (2008) 441–449, DOI: 10.1016/j.ijpvp.2008.01.006.
[26] G. Mathan, N. Prasad, Study of dynamic response of piping system with gasketed flanged joints using finite element analysis, International Journal of Pressure Vessels and Piping 89 (2012) 28–32, DOI: 10.1016/j.ijpvp.2011.09.002.
[27] C. Schwingshackl, E. Petrov, Modeling of flange joints for the nonlinear dynamic analysis of gas turbine engine casings, Journal of Engineering for Gas Turbines and Power, Transactions of the ASME 134 (12) (2012) art. no. 122504, DOI: 10.1115/1.4007342.
[28] L. Shuguo, M. Yanhong, Z. Dayi, H. Jie, Studies on dynamic characteristics of the joint in the aero-engine rotor system, Mechanical Systems and Signal Processing 29 (2012) 120–136, DOI: 10.1016/j.ymssp.2011.12.001.
[29] T. Do, A.-H. Bouzid, T.-M. Dao, Development of a new bolt spacing formula, Journal of Pressure Vessel Technology, Transactions of the ASME 136 (1) (2014) Article number 011206, DOI: 10.1115/1.4025613.
[30] T. Nakamura, K. Funabashi, Effects of directional properties of roughness and tangential force on pressure flow between contacting surfaces, Lubrication Science 4 (1) (1991) 13–23.
[31] G. Murtagian, V. Fanelli, J. Villasante, D. Johnson, H. Ernst, Sealability of Stationary Metal-to-Metal Seals, Journal of Tribology, Transactions of the ASME 126 (3) (2004) 591–596, DOI: 10.1115/1.1715103.
[32] Y. Ledoux, D. Lasseux, H. Favreliere, S. Samper, J. Grandjean, On the dependence of static flat seal efficiency to surface defects, International Journal of Pressure Vessels and Piping 88 (11–12) (2011) 518–529, DOI: 10.1016/j.ijpvp.2011.06.002.
[33] H. Kawamura, T. Sawa, M. Yoneno, FEM stress analysis and sealing performance improvement of box-shaped bolted flanged joints using silicone sealant under internal pressure and thermal conduction conditions, Journal of Adhesion Science and Technology 17 (8) (2003) 1109–1125, DOI: 10.1163/156856103322113823.
[34] A. Müller, W. Becker, D. Stolten, J. Hohe, A hybrid method to assess interface debonding by finite fracture mechanics, Engineering Fracture Mechanics 73 (8) (2006) 994–1008, DOI: 10.1016/j.engfracmech.2005.12.001.
[35] H. Tsuji, M. Nakano, Bolt preload control for bolted flange joint, in: American Society of Mechanical Engineers, Pressure Vessels and Piping Division (Publication) PVP, 433, 2002, pp. 163–170, vancouver, BC, Canada, Paper 1094.
[36] T. Fukuoka, T. Takaki, Elastic Plastic Finite Element Analysis of Bolted Joint During Tightening Process, Journal of Mechanical

Design, Transactions of the ASME 125 (4) (2003) 823–830, DOI: 10.1115/1.1631579.
[37] T. Fukuoka, T. Takaki, Finite Element Simulation of Bolt-Up Process of Pipe Flange Connections With Spiral Wound Gasket, Journal of Pressure Vessel Technology, Transactions of the ASME 125 (4) (2003) 371–378, DOI: 10.1115/1.1613304.
[38] T. Fukuoka, Finite Element Analysis of the Thermal and Mechanical Behaviors of a Bolted Joint, Journal of Pressure Vessel Technology, Transactions of the ASME 127 (4) (2005) 402–407, DOI: 10.1115/1.2042477.
[39] L. Bertini, M. Beghini, C. Santus, G. Mariotti, Metal to metal flanges leakage analysis, American Society of Mechanical Engineers, Pressure Vessels and Piping Division (Publication) PVP 6 (PART A) (2010) 149–158, Proceedings of the 2009 ASME Pressure Vessels and Piping Conference. PVP2009-77730. DOI: 10.1115/PVP2009-77730.
[40] M. Beghini, L. Bertini, V. Fontanari, Weight Function for an Inclined Edge Crack in a Semiplane , International Journal of Fracture 99 (4) (1999) 281–292.
[41] M. Beghini, L. Bertini, Effective stress intensity factor and contact stress for a partially closed Griffith crack in bending, Engineering Fracture Mechanics 54 (5) (1996) 667–678, DOI: 10.1016/0013-7944(95)00234-0.
[42] M. Beghini, L. Bertini, V. Fontanari, A weight function technique for partially closed inclined edge cracks analysis, International Journal of Fracture 112 (1) (2001) 57–68, DOI: 10.1023/A:1013529608424.
[43] M. Beghini, L. Bertini, V. Fontanari, Parametric study of oblique edge cracks under cyclic contact loading, Fatigue & Fracture of Engineering Materials & Structures 28 (1–2) (2005) 31–40, DOI: 10.1111/j.1460-2695.2004.00860.x.
[44] V. Kahya, A. Birinci, T. Ozsahin, R. Erdol, Partial closure of a crack located in an anisotropic infinite elastic layer, European Journal of Mechanics, A/Solids 25 (5) (2006) 819–833, DOI: 10.1016/j.euromechsol.2006.01.005.
[45] A. Birinci, F. Birinci, F. Cakiroglu, R. Erdol, An internal crack problem for an infinite elastic layer, Archive of Applied Mechanics 80 (9) (2010) 997–1005, DOI: 10.1007/s00419-009-0355-5.
[46] X.-R. Wu, A. Carlsson, Weight Functions and Stress Intensity Factor Solutions, Pergamon Press, Oxford, 1991.
[47] T. Fett, D. Munz, Stress Intensity Factors and Weight Functions, Computational Mechanics Publications, 1997.
[48] M. Beghini, C. Santus., An application of the weight function technique to inclined surface cracks under rolling contact fatigue, assessment and parametric analysis, Engineering Fracture Mechanics 98 (2013) 153–168, DOI: 10.1016/j.engfracmech.2012.10.024.
[49] R. Budynas, K. Nisbett, Shigley's Mechanical Engineering Design, 9th Edition, McGraw-Hill Science/Engineering/Math, 2010.
[50] J. Mackerle, Fastening and joining: finite element and boundary element analyses - A bibliography (1992-1994), Finite Elements in Analysis and Design 20 (3) (1995) 205–215.
[51] J. Mackerle, Finite element analysis of fastening and joining: A bibliography (1990-2002), International Journal of Pressure Vessels and Piping 80 (4) (2003) 253–271, DOI: 10.1016/S0308-0161(03)00030-9.
[52] J. Mackerle, Finite elements in the analysis of pressure vessels and piping, an addendum: A bibliography (2001-2004), International Journal of Pressure Vessels and Piping 82 (7) (2005) 571–592, DOI: 10.1016/j.ijpvp.2004.12.004.
[53] M. Abasolo, J. Aguirrebeitia, R. Avilés, I. F. de Bustos, A Tetraparametric Metamodel for the Analysis and Design of Bolting Sequences for Wind Generator Flanges, Journal of Pressure Vessel Technology, Transactions of the ASME 133 (4) (2011) art. no. 041202, DOI: 10.1115/1.4002541.
[54] J. Kim, J.-C. Yoon, B.-S. Kang, Finite element analysis and modeling of structure with bolted joints, Applied Mathematical Modelling 31 (5) (2007) 895–911, DOI: 10.1016/j.apm.2006.03.020.
[55] R. Oskouei, M. Keikhosravy, C. Soutis, A finite element stress analysis of aircraft bolted joints loaded in tension, Aeronautical Journal 114 (1155) (2010) 315–320.
[56] F. Gant, P. Rouch, F. Louf, L. Champaney, Definition and updating of simplified models of joint stiffness, International Journal of Solids and Structures 48 (5) (2011) 775–784, DOI: 10.1016/j.ijsolstr.2010.11.011.
[57] I. Uysal, M. Süer, I. Ozkol, Finite element modelling and analysis of simple lap joints, in: RAST 2011 - Proceedings of 5th International Conference on Recent Advances in Space Technologies, art. no. 5966925, 2011, pp. 68–72, DOI: 10.1109/RAST.2011.5966925.
[58] I. Korin, J. P. Ipiña, Experimental evaluation of fatigue life and fatigue crack growth in a tension bolt-nut threaded connection, International Journal of Fatigue 33 (2) (2011) 166–175, DOI: 10.1016/j.ijfatigue.2010.08.003.
[59] S. Izumi, T. Yokoyama, M. Kimura, S. Sakai, Loosening-resistance evaluation of double-nut tightening method and spring washer by three-dimensional finite element analysis, Engineering Failure Analysis 16 (5) (2009) 1510–1519, DOI: 10.1016/j.engfailanal.2008.09.027.
[60] G. Dinger, C. Friedrich, Avoiding self-loosening failure of bolted joints with numerical assessment of local contact state, Engineering Failure Analysis 18 (8) (2011) 2188–2200, DOI: 10.1016/j.engfailanal.2011.07.012.
[61] T. Yokoyama, M. Olsson, S. Izumi, S. Sakai, Investigation into the self-loosening behavior of bolted joint subjected to rotational loading, Engineering Failure Analysis 23 (2012) 35–43, DOI: 10.1016/j.engfailanal.2012.01.010.
[62] H. Estrada, I. Parsons, Strength and leakage finite element analysis of a GFRP flange joint, International Journal of Pressure Vessels and Piping 76 (8) (1999) 543–550, DOI: 10.1016/S0308-0161(99)00021-6.
[63] J. Williams, R. Anley, D. Nash, T. Gray, Analysis of externally loaded bolted joints: Analytical, computational and experimental study, International Journal of Pressure Vessels and Piping 86 (7) (2009) 420–427, DOI: 10.1016/j.ijpvp.2009.01.006.
[64] X. Zheng, W. Xia, Numerical simulation of blind hole bolt connection with 3-D finite element approach, in: 2nd International Conference on Information and Computing Science, ICIC 2009, Vol. 4, art. no. 5169152, 2009, pp. 164–169, DOI: 10.1109/ICIC.2009.352.

Appendix. Calculation procedure for nominal stresses

Leakage pressure Eq. 12 can be easily solved with the unitary nominal stresses $\sigma_{n,B1}(0), \sigma_{n,B1}(L)$ and $\sigma_{n,p1}(0), \sigma_{n,p1}(L)$. Below is a procedure to calculate these stresses from the flange parameters.
Initially, the following geometry definitions are introduced:

$$\begin{aligned}
&\alpha = 35^\circ = 0.6109 \text{ rad} \\
&L = Z - d_H/2 \\
&\text{Bolt: } D_0 = d_N + 2H\tan(\alpha) \\
&\text{Stud: } D_0 = \min\{d_N + 2H\tan(\alpha); d_H + 2(H_S + 2d_t - H)\tan(\alpha)\} \\
&L' = (D_0 - d_H)/2 \\
&W' = \min\{W; Z + d_H/2 + L'\}
\end{aligned} \tag{15}$$

D_0 is the flange contact overall width induced by bolt or stud. Specifically for studded flanges, D_0 is usually limited by the depth of the stud thread (right hand side term for D_0), unless the thickness of the flange upper plate is significantly smaller than the other plate, and d_t is the thread diameter of the stud from where the compressive zone widens. L' is the net contact width after subtracting the hole diameter d_H, and W' is the width the pressure distribution is acting on, possibly limited by the external end side.
After the calculation of d'_H from Eq. 9, the contact area, the centroid and the second moment of area can be obtained as the following:

$$\begin{aligned}
&A_W = P_B W' - \pi/4\, d_H^2 \\
&x_W = (P_B W'^2/2 - \pi/4\, d_H^2 Z)/A_W \\
&I_W = (1/12\, P_B W'^3 + P_B W'(x_W - W'/2)^2) - (\pi/64\, d_H^4 + \pi/4\, d_H^2 (x_W - Z)^2)
\end{aligned} \tag{16}$$

Given that the bolt stress is $\sigma_B = F_B/\frac{\pi}{4}d_B^2$, the unitary bolt preload is the corresponding force with $\sigma_B = 1$:

$$F_{B1} = \frac{\pi}{4} d_B^2 \tag{17}$$

The trapezoidal nominal stress (or opposite sign pressure) initially calculated with no redistribution (NR) is:

$$\sigma_{n,B1}^{NR} = -\frac{F_{B1}}{P_B(L' + d_H - d'_H)} \tag{18}$$

This stress then needs to be redistributed according to Fig. 6 (a). First if the pressure at the inner side is zero, the proposed calculation is not possible. The condition to be verified is: $L < L'$, however, vessel geometries usually have this condition well satisfied. The forces F_1, F_2 (with unitary bolt stress) need to be calculated along with their moments:

$$\begin{aligned}
&F_1 = \sigma_{n,B1}^{NR} P_B (1 - L/L')(L' - L)/2 \\
&M_1 = F_1((L' - L)/3 + x_W) \\
&L_2 = W' - (L + d_H) \\
&F_2 = \sigma_{n,B1}^{NR} P_B (1 - L_2/L')(L' - L_2)/2 \\
&M_2 = -F_2(W' + (L' - L_2)/3 - x_W) \\
&F_{12} = F_1 + F_2 \\
&M_{12} = M_1 + M_2
\end{aligned} \tag{19}$$

When $W' = Z + d_H/2 + L'$ (i.e. the flange width is relatively long: $W > Z + d_H/2 + L'$) it follows that $L_2 = L'$ and then F_2 is zero as well as its moment M_2. Now the nominal stresses can be obtained including the redistribution forces F_1, F_2:

$$\begin{aligned}
&\sigma_{n,B1}^{t} = F_{12}/A_W \\
&\sigma_{n,B1}^{b}(0) = M_{12} x_W / I_W \\
&\sigma_{n,B1}^{b}(L) = M_{12}(x_W - L)/I_W \\
&\sigma_{n,B1}(0) = \sigma_{n,B1}^{NR}(1 - L/L') + \sigma_{n,B1}^{t} + \sigma_{n,B1}^{b}(0) \\
&\sigma_{n,B1}(L) = \sigma_{n,B1}^{NR} + \sigma_{n,B1}^{t} + \sigma_{n,B1}^{b}(L)
\end{aligned} \tag{20}$$

where: $\sigma^{t}_{n,B1}, \sigma^{b}_{n,B1}$ are the tensile and the bending component, respectively, to be superimposed.
Finally, the unitary internal pressure nominal stresses can be easily calculated since the geometry parameters are already available:

$$\begin{aligned}
&F_{p1} = P_B D_V/2 \\
&\sigma^{t}_{n,p1} = F_{p1}/A_W \\
&\sigma^{b}_{n,p1}(0) = F_{p1}(x_W - t_V/2)x_W/I_W \\
&\sigma^{b}_{n,p1}(L) = F_{p1}(x_W - t_V/2)(x_W - L)/I_W \\
&\sigma_{n,p1}(0) = \sigma^{t}_{n,p1} + \sigma^{b}_{n,p1}(0) \\
&\sigma_{n,p1}(L) = \sigma^{t}_{n,p1} + \sigma^{b}_{n,p1}(L)
\end{aligned} \tag{21}$$

Equations 20, 21 provide the four terms $\sigma_{n,B1}(0), \sigma_{n,B1}(L)$ and $\sigma_{n,p1}(0), \sigma_{n,p1}(L)$ to be inputted in Eq. 12.

List of Figures

List of Tables

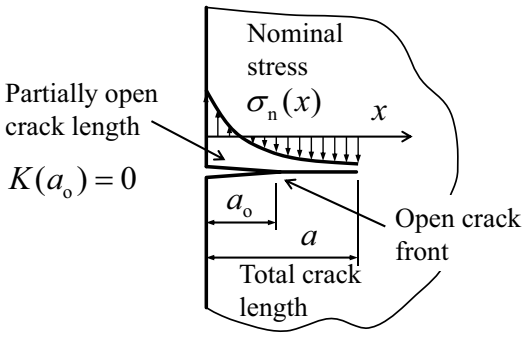

Figure 1: Nominal stress with a compressive region which causes a partially open crack.

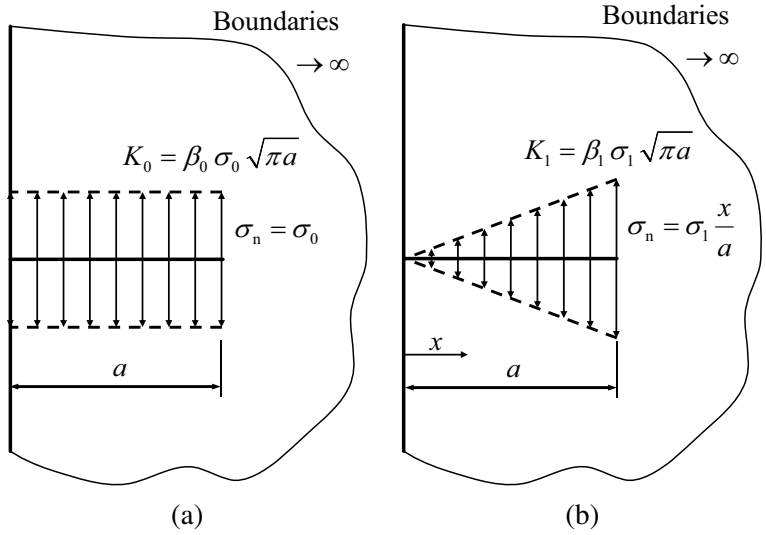

Figure 2: Weight Function integrations: (a) uniform nominal stress, (b) linear nominal stress with zero at the surface edge.

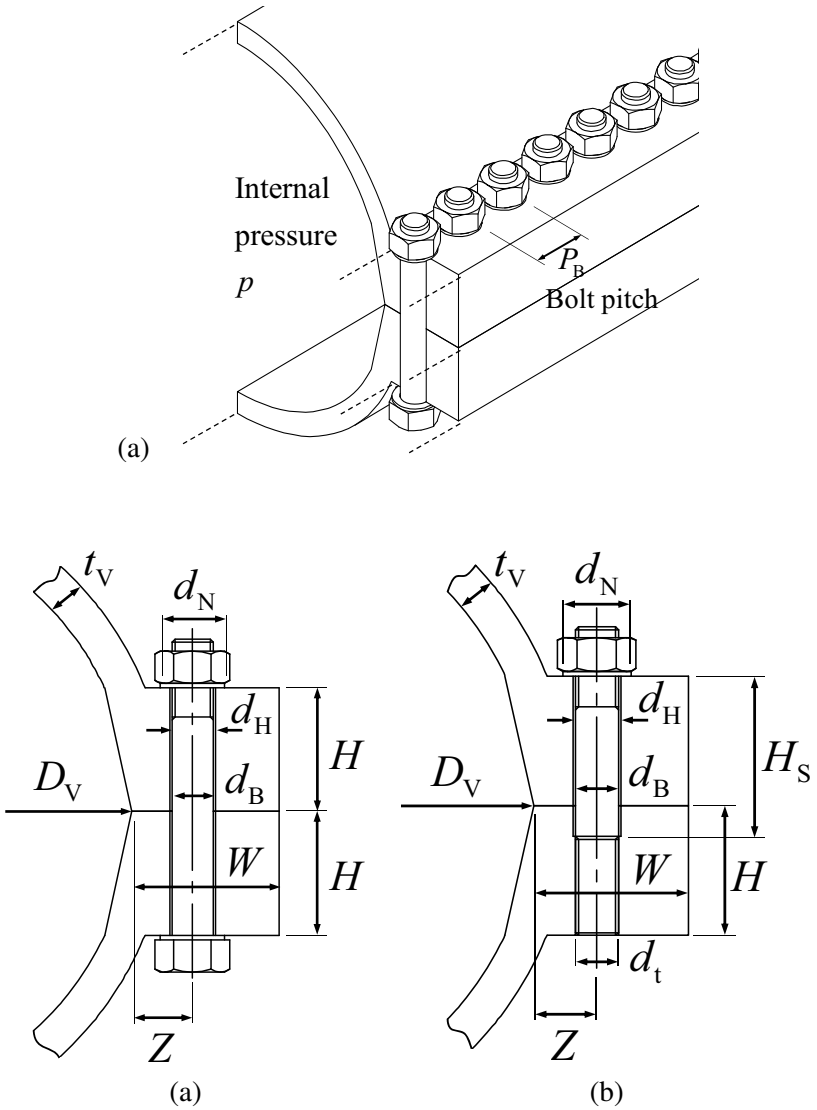

Figure 3: Geometry parameters: bolted (a) and studded (b) flanges.

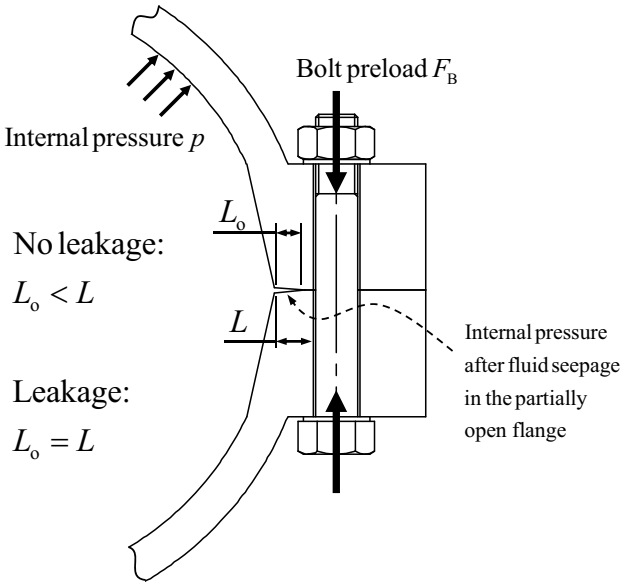

Figure 4: Flange leakage condition.

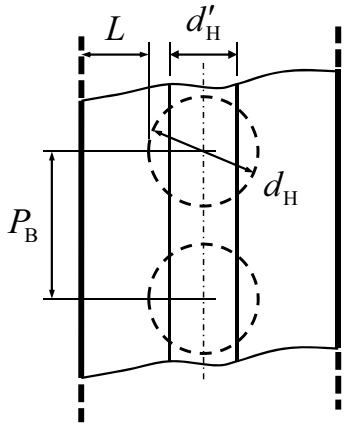

Figure 5: Bolt hole sequence equivalent to a continuous slot.

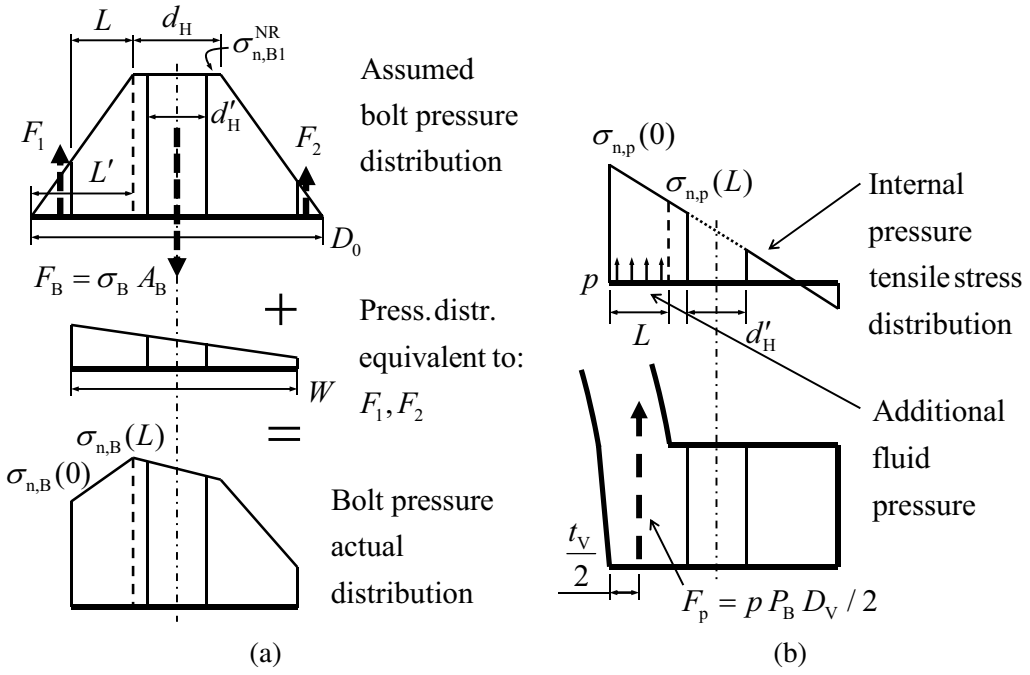

Figure 6: Nominal stress distributions: bolt preload (a), internal pressure (b).

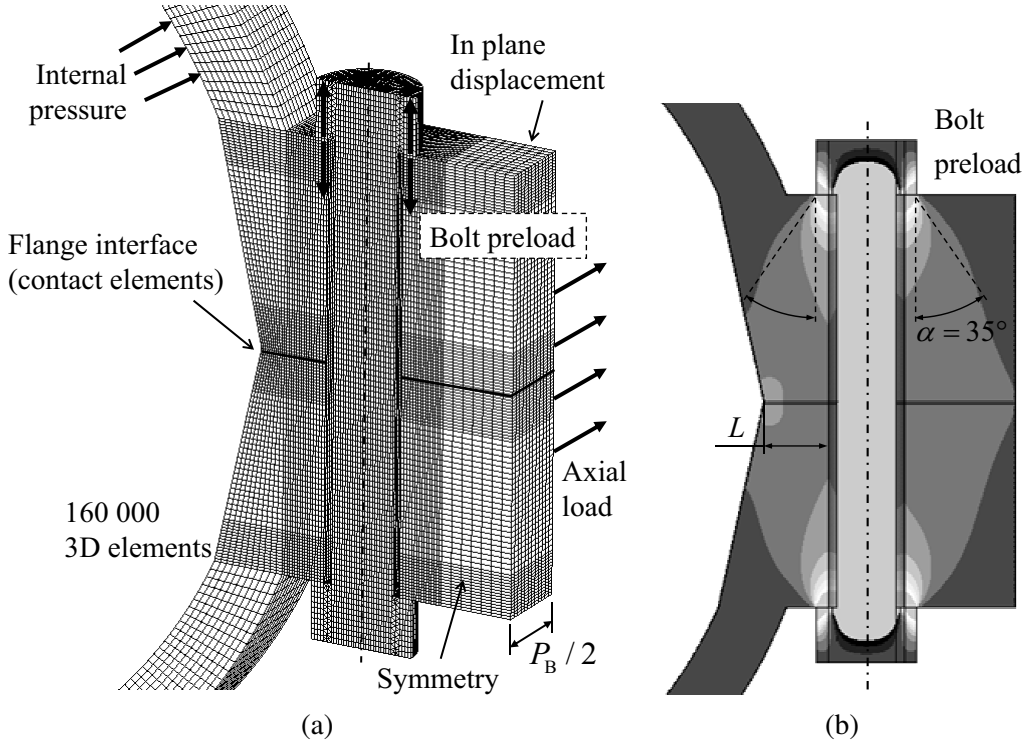

Figure 7: (a) Loads and constraints applied to the FE model. (b) Stress distribution induced by the bolt preload alone, before applying internal pressure.

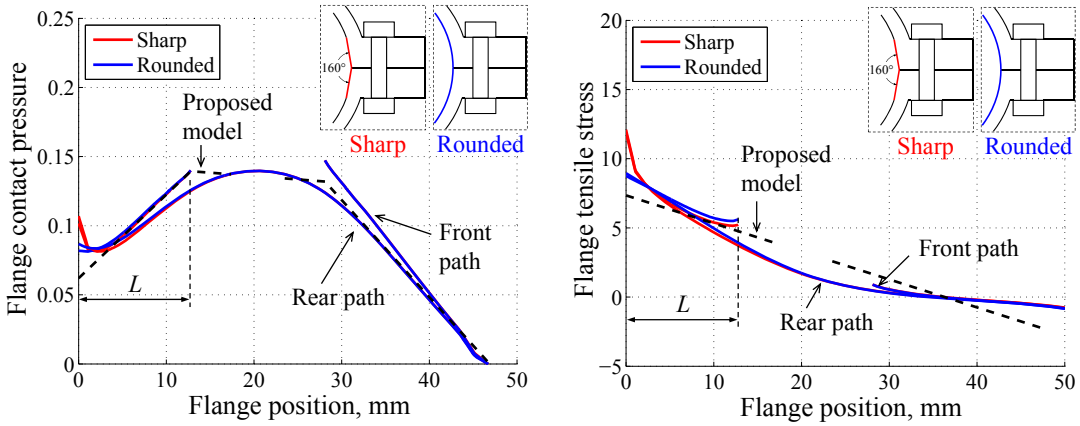

Figure 8: Nominal stresses induced by unitary bolt preload (a) and unitary internal pressure (b). Comparison between the analytical and the FE models and effect of the internal edge geometry.

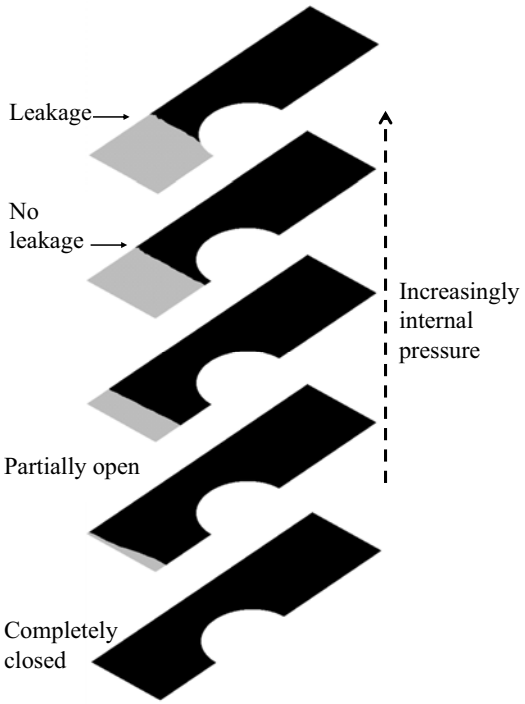

Figure 9: Determination of the FE model leakage pressure.

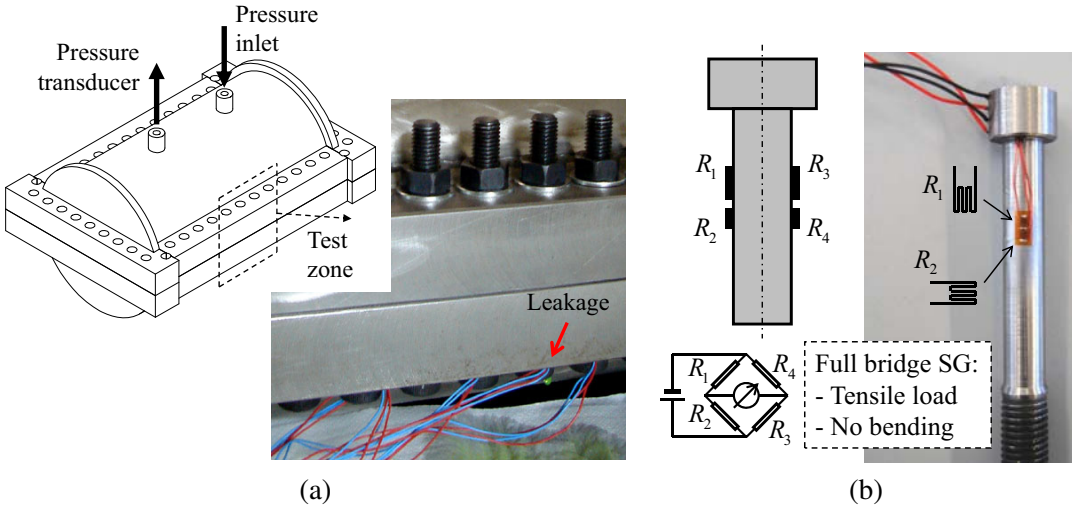

Figure 10: (a) Small scale vessel pressurization test and leakage detection. (b) Bolt with full-bridge configuration strain gauges.

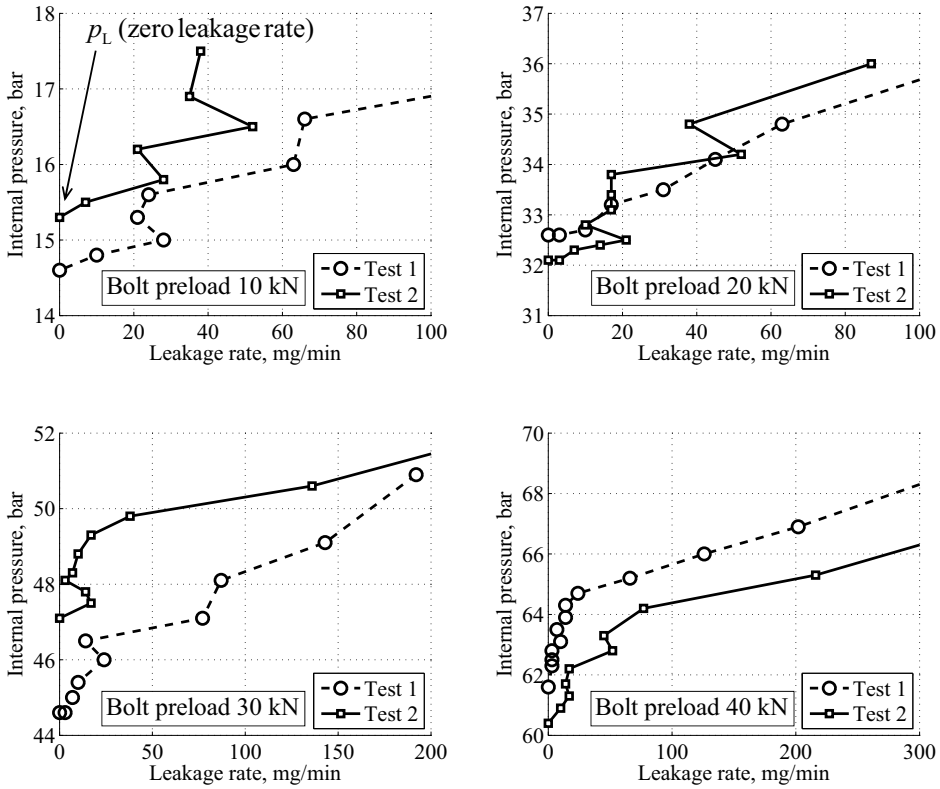

Figure 11: Leakage rates for different bolt preloads and detection of the leakage pressures.

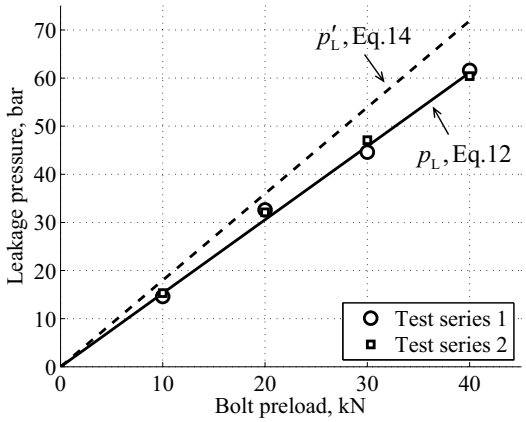

Figure 12: Comparison between the experimental results and the analytical model predictions.

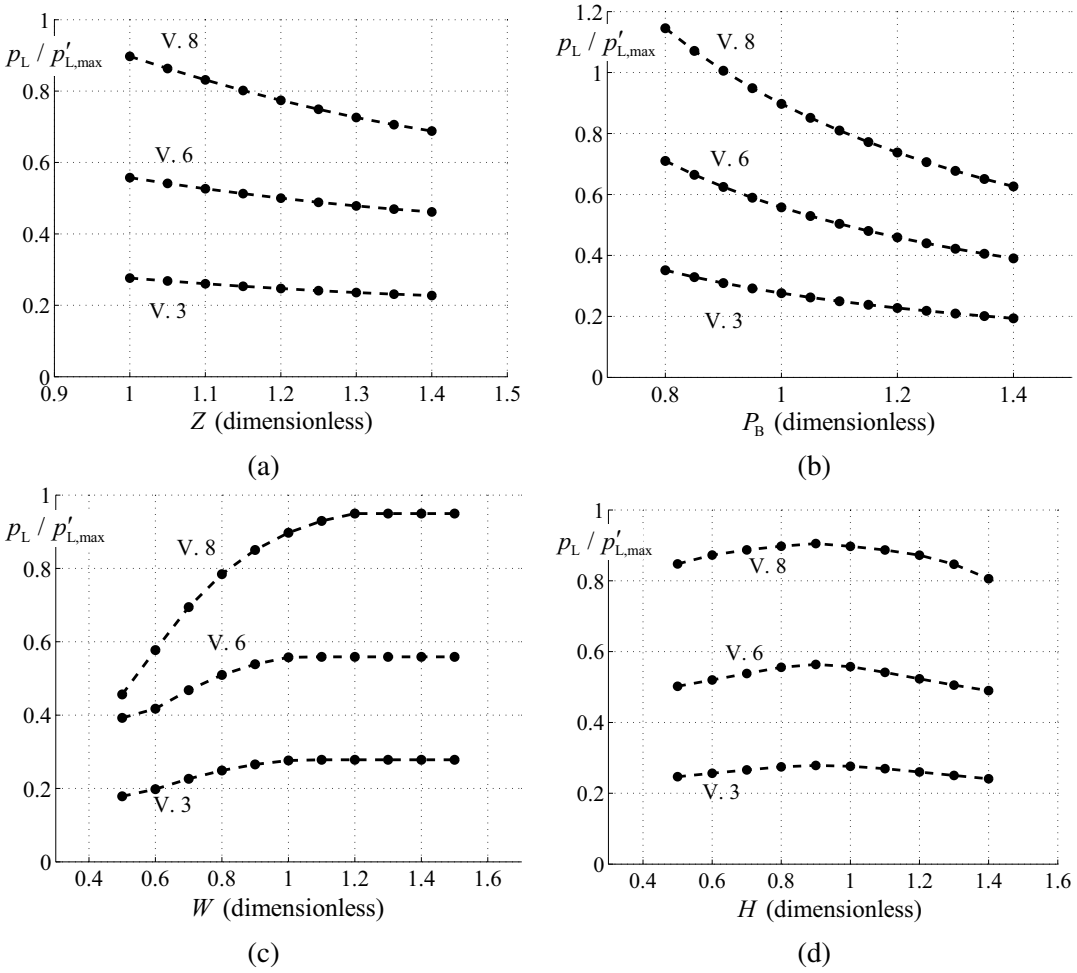

Figure 13: Leakage pressure sensitivity: bolt axis position (a), bolt pitch (b), flange width (c), and flange height (d).

Vessel	D_V/t_V	W/t_V	H/t_V	Z/t_V	P_B/t_V	d_B/t_V	d_H/t_V	$\frac{p_L}{p'_L}$	$\frac{p'_L}{p'_{L,max}}$	$\frac{p'_{L,FE}}{p'_{L,max}}$	$\Delta p', \%$
1, stud	28.8	3.880	3.120	1.641	2.301	1.132	1.248	0.91	0.827	0.830	$-0.3\,\%$
2, stud	28.3	4.571	3.486	1.614	2.306	1.200	1.286	0.91	0.512	0.519	$-1.5\,\%$
3, stud	37.5	4.500	3.050	1.663	2.275	1.050	1.125	0.93	0.291	0.284	$2.3\,\%$
4, stud	33.6	4.455	3.127	1.545	1.849	0.782	0.945	0.92	0.433	0.452	$-4.2\,\%$
5, stud	22.6	3.826	3.130	1.496	2.233	1.035	1.139	0.89	0.920	0.915	$0.5\,\%$
6, stud	28.9	4.000	2.867	1.467	1.768	0.733	0.944	0.91	0.595	0.592	$0.4\,\%$
7, stud	28.8	3.880	3.040	1.560	2.209	1.012	1.128	0.91	0.699	0.684	$2.2\,\%$
8, stud	22.2	3.704	3.259	1.444	2.148	1.048	1.156	0.90	1.000	1.027	$-2.6\,\%$
9, stud	41.1	4.889	3.156	1.689	2.148	0.956	1.156	0.93	0.460	0.458	$0.5\,\%$
10, stud	27.8	4.300	3.040	1.670	2.544	1.000	1.200	0.90	0.629	0.597	$5.5\,\%$
11, stud	34.0	4.300	2.850	1.580	2.234	0.940	1.060	0.92	0.508	0.490	$3.7\,\%$
12, stud	50.0	4.167	2.833	1.667	1.691	0.717	0.867	0.94	0.263	0.260	$1.0\,\%$
13, stud	35.2	4.417	3.000	1.575	2.230	0.967	1.133	0.93	0.528	0.524	$0.7\,\%$
14, bolt	16.0	4.032	3.336	1.636	2.400	0.960	1.224	0.85	0.268	0.265	$1.1\,\%$

Table 1: Dimensionless vessel geometry parameters and leakage pressure results.